JOURNAL OF CATALYSIS 24, 18-39 (1972)

The Poisoning of a Steam Hydrocarbon Gasification Catalyst

F. MOSELEY, R. W. STEPHENS, K. D. STEWART, AND J. WOOD

The Gas Council, Midlands Research Station, Wharf Lane, Solihull, Warwickshire, England

Received September 22, 1970

The factors which affect the loss of activity of a nickel alumina catalyst for the gasification of sulfur-free light hydrocarbons with steam at temperatures below 500°C have been examined. These are sintering or loss of active surface area due to heat treatment in steam, and poisoning of active sites by a much slower parallel reaction to gasification involving constituents of the hydrocarbon feedstock. The second of these modes of activity loss is much more important at temperatures between 400 and 500°C and normal operating pressures around 25 atm. This second mode of poisoning is independent of total pressure but rises rapidly with the boiling point of the hydrocarbon feedstock and the hydrocarbon steam ratio supplied. Increases in temperature favor the gasification reaction at the expense of poisoning.

With finely divided catalyst particles, the rate of the gasification reaction is chemically controlled and zero order with respect to steam and hydrocarbon. With larger particles (0.3 cm diam) the rate is controlled by gaseous diffusion in the pores of the catalyst and, in line with this, the reaction rate becomes proportional to the particle size, the reaction order rises, and the activation energy falls. Rate control is probably by Knudsen diffusion in the micropores, though bulk diffusion in the macropores cannot be ruled out. The poisoning rate falls sharply at first on entering the region of diffusional control as the particle diameter is increased, but ultimately becomes independent of size. An attempt is made to interpret this phenomenon in terms of the effects of diffusional rate control on steam hydrocarbon ratio and temperature.

INTRODUCTION

During the last 14 years, several catalytic processes have been developed for the conversion of light hydrocarbon oils by reaction with steam to mixtures of methane, carbon monoxide, carbon dioxide, and hydrogen. Among these is the Gas Council "CRG" process developed in these laboratories (*1*), in which steam and light petroleum distillate in weight ratios commonly between 1.6 and 2 to 1 are supplied to an active catalyst bed on which gasification occurs at high space velocity, typically at inlet temperatures of around 450°C and pressures of 25 atm. If the catalyst is sufficiently active, all hydrocarbons other than methane are decomposed in due course and the product gases are in thermodynamic equilibrium at the exit temperature according to the two equations:

$$CO + 3H_2 = CH_4 + H_2O, \qquad (1)$$

$$CO_2 + H_2 = CO + H_2O. \qquad (2)$$

At these inlet temperatures and pressures, the gases leave the reactor generally 50-80°C hotter if no heat loss occurs, the overall reactions which take place being slightly exothermic. The increase in temperature between inlet and outlet is greater at high pressures because increased pressure drives reaction (1) to the right, yields a higher percentage of methane in the equilibrium gases for a given steam hydrocarbon feed ratio, and liberates more heat, since the formation of methane by this reaction is highly exothermic.

The hydrocarbon feedstock reacts progressively as it passes through the catalyst and this gives rise to a temperature profile through the bed of the type illustrated in Fig. 1. In this example, the steam hydrocarbon mixture enters at 450°C and initially the temperature falls slightly as hydrocarbon decomposition and reaction with steam begin, because the very high partial pressure of unreacted steam maintains reaction (1) well to the left and the small amount of reaction is endothermic overall. As decomposition proceeds, steam is removed nett and the reaction swings past the "thermoneutral point," finally yielding a temperature over 70°C in excess of the initial feed gas temperature when decomposition and equilibration of the products is complete.

Profiles of this type can be predicted by calculation (*2*) assuming that, at each stage of the reaction, undecomposed hydrocarbons other than methane behave as inert gases and that the equilibria expressed by Eqs. (1) and (2) are attained among the products. Experimental work on powdered catalysts (*2*) has shown that this assumption is not quite correct and that excess hydrogen and carbon monoxide are present with partially reacted distillate, but the small errors introduced in the heat balance by the assumption of equilibrium are not large enough to prevent a satisfactory agreement as to general shape between calculated and experimental profiles.

In this paper, use has been made of this profile to examine the factors which influence the loss of activity of a typical nickel gasification catalyst. For a given feed ratio, feed temperature, hydrocarbon, and pressure, a certain fraction of the hydrocarbon supplied is decomposed at the thermoneutral point. In an adiabatic reactor, therefore, monitoring the progression of the thermoneutral point through the bed with time provides a laboratory method of observing the loss of activity or poisoning of the catalyst. Furthermore, the rate of progression of the thermoneutral point will adequately represent loss of activity, even at different pressures of operation or feed ratios where the "point" will not be at quite the same fractional conversion, provided the time taken for a catalyst to lose activity is long compared with the "residence time" to achieve full conversion of feedstock.

The method is simple experimentally and closely represents the circumstances in which the catalyst would be used on the large scale. The conclusions reached are, however, qualitative because inevitably in such a system there is no control over the reaction temperature distribution and its change with conversion or catalyst poisoning. Isothermal operation was not attempted

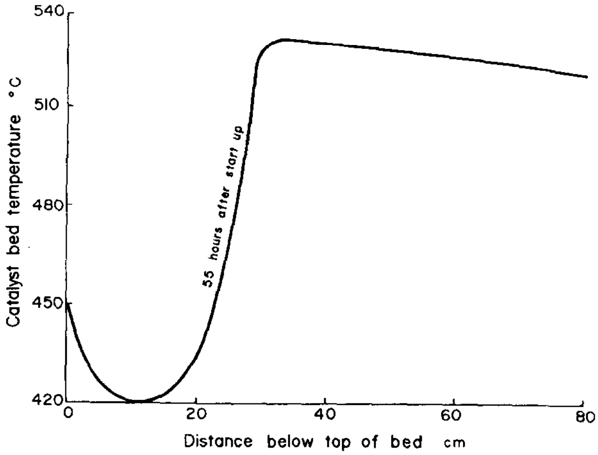

FIG. 1. Reaction temperature profile through 1.3 cm i.d. catalyst bed: catalyst bed 84 × 1.3 cm of 18–30 BSS particles; water feed rate, 530 g/hr; distillate feed rate, 320 g/hr; distillate final boiling point, 170°C; pressure, 25 atm; initial inlet gas and reactor temperatures, 450°C.

because temperature control is extremely difficult with active catalyst, even with catalyst dilution and massive addition of inert carrier gas.

EXPERIMENTAL METHODS

The laboratory apparatus (Fig. 2) was designed to simulate as closely as possible the virtually adiabatic operation of large plant. Sulfur-free (<0.1 ppm) light petroleum distillate delivered at pressure by metering pump A was vaporized in a stainless-steel tube passing through a heated aluminium block B held at a controlled temperature of 280°C. Water was supplied by a similar pump C, converted to steam in evaporator D and mixed with the vaporized distillate at E in a stainless-steel tube wrapped with a heating tape. A pressure gauge P_1 and a supply tube for other gases were located at F. The mixture of gases passed on through a controlled temperature aluminium block preheater G, 23 cm long, in which it was brought to the desired temperature, and thence to the reactor. The stainless-steel reactor tube I, usually 46 or 92 cm long, was 0.44 cm i.d. and 0.67 cm o.d. It was lagged with asbestos rope to an overall diameter of 5 cm to minimize heat gain or loss and the whole was contained in an electric furnace H with three separately controlled windings, at the entrance, in the middle, and at the exit.

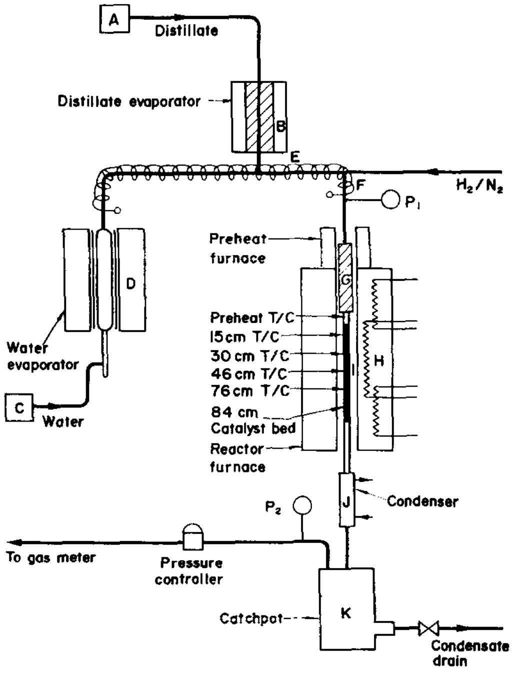

FIG. 2. Diagram of apparatus used in laboratory tests.

Catalyst, either as pellets or powder, was packed into the reactor where it rested on a wire mesh plate in the tube at the outlet end. Bed depths used were usually 38 or 84 cm. Six fine chromel–alumel thermocouples were strapped to the outside of the reactor tube. The first was located 2.5 cm above the catalyst bed to record the preheat temperature; when a 46 cm reactor was used, the others were 10, 15, 23, 30, and 36 cm from the top of the bed and at 15, 30, 46, 61, and 76 cm when the reactor was 92 cm long.

Preliminary experiments were generally made in 38 cm beds to save time, although even these could last well over a week. Experience showed that because of a number of factors, described below, these beds were not long enough to provide more than qualitatively comparable data on poisoning under some conditions of operation. Where thought necessary, the experiments were repeated in 84 cm beds.

The temperatures indicated by the six thermocouples were monitored on the chart of a six-point recorder. Occasionally beds of larger diameter were used, which were fitted with a narrow central internal tube which contained one movable thermocouple.

Gases emerging from the reactor were passed through a water-cooled condenser J to a catch pot K in which unreacted steam was collected as water, thence they passed to an automatic release valve L which controlled the plant pressure, where they were reduced to atmospheric pressure and passed to a wet gas meter. The catch pot was fitted with an automatic drainage valve which opened and closed between preset liquid levels in the catch pot. An outlet pressure gauge P_2 was attached to the pot. The whole apparatus was shut down automatically by a pressure switch if a preset pressure at the inlet was exceeded. Gas samples were taken for analysis by both Bone and

Wheeler and gas chromatographic methods.

The gasification catalyst (composition 75 wt % nickel, 25 wt % alumina doped with 0.6% potassium) was made by precipitation of nickel carbonate and alumina from a hot solution of nickel nitrate and aluminium nitrate using 15 wt % potassium carbonate solution. The precipitate was washed with distilled water until neutral, the cake was stirred with a solution of potassium carbonate containing sufficient potassium to produce 0.6% by wt in the final product, the whole was dried and finally heated to 450°C for 8 hr. The fired catalyst was pressed to form 0.32 cm equant cylindrical pellets with 2% graphite addition to act as lubricant. These pellets were used direct in some experiments; other catalyst particles with sieve sizes of 6–8, 8–10, 10–14, 18–30, and 36–52 BSS were prepared from them by grinding and sieving. Some 0.64 cm equant cylindrical pellets were also made. All the laboratory scale experiments reported in this paper were made on the catalyst prepared in one precipitation.

The start-up procedure was as follows. The reactor tube was packed with catalyst, the plant was pressurized with nitrogen and then, with a flow of nitrogen roughly equivalent to the flow of steam which would be used, the furnace windings and preheater were adjusted to give a uniform temperature (±1°C) of usually 450°C along the whole length of preheater and reactor tube. Nitrogen was then replaced by hydrogen supplied for 4 hr at 60 liters/hr to reduce the catalyst. Steam flow was started at the desired rate and maintained for 1 hr, when the hydrogen flow was stopped and distillate supply was commenced. Zero time was taken as the instant when distillate pumping began and the temperature profile and movement of the profile through the bed with time was observed. Each thermocouple in turn from the top of the bed recorded first an increase in temperature above the original recorded, then as catalyst activity was lost the temperature fell, eventually going below the original temperature and finally, when all activity had been lost by the catalyst in front of the thermocouple, returning yet again to the original preset temperature. The time taken for each thermocouple to return to its original temperature for the first time was noted and these times were plotted against the distance of the thermocouple from the beginning of the bed. Alternatively, with a known packing density and a known and constant distillate supply rate, the results could be replotted in the form of graphs of the amount of distillate supplied against the number of grams of catalyst originally charged which had been deactivated.

In addition, some results obtained from experiments made in 5 cm diameter reactors with longer beds have been reported (*3*). These were obtained in the course of scaling up the process for industrial use. Data from these reactors had the advantage that operation was more closely adiabatic since the throughput/reactor surface area ratio was so much bigger.

RESULTS

1. The Shape of the Deactivation Plot

Figure 3 shows the result of a typical experiment in which the time for each thermocouple to record the thermoneutral point is plotted against its distance from the beginning of the bed, and Fig. 4, the shape of the temperature profiles at various times from start-up. The conditions were: original temperature, 450°C; pressure, 25 atm; steam supply rate, 65 g/hr; steam: distillate weight ratio in feed, 1.66:1; distillate final boiling point, 170°C; catalyst charged to 84 cm bed, 11.2 g.

Figure 4 shows that the temperature profile does not change much in shape as it progresses through the bed with time, except that the endothermic region tends to increase in length, indicating that the catalyst at the bed entrance is slow to lose its last remaining traces of activity. The much larger fall in temperature after the maximum which occurs with the narrow bore 0.44 cm tube when compared to Fig. 1 is a result of the greater heat loss to the furnace at 450°C after completion of the reaction. Figure 3 is a curve which tends slowly to a straight line, but the loss of activity it

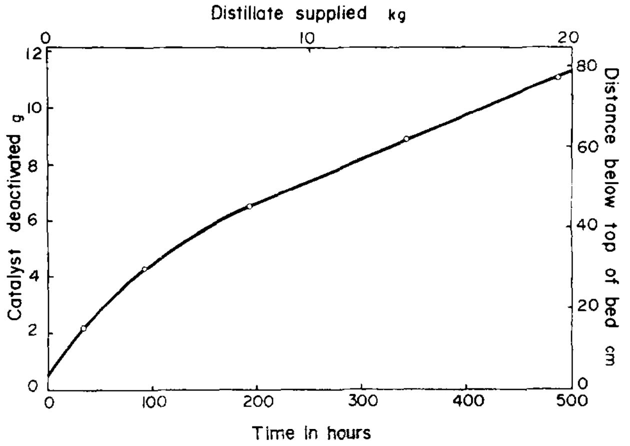

FIG. 3. Typical poisoning or deactivation curve: catalyst bed 84 × 0.44 cm of 18–30 BSS particles; weight of charge, 12.7 g before reduction; water feed rate, 65 g/hr; distillate feed rate, 39 g/hr; distillate final boiling point, 170°C; pressure, 25 atm: initial inlet gas and reactor temperature, 450°C.

represents is influenced by a number of factors, particularly in the early stages.

Firstly catalyst in the small section at the entrance of the bed has a lower average temperature over time than subsequent sections. This is because the reaction zone, as represented by the temperature profile, has a finite length at full catalyst activity or zero time whose initial portion has a lower temperature than the original set temperature; whereas the remainder of the bed is at higher temperature. It can be presumed that the rate of the poisoning reaction is influenced by temperature, so that the average poisoning rate will be different for the small section of bed at the entrance.

Secondly there is the phenomenon of sintering. It is known that nickel on γ-alumina catalysts lose surface area or sinter with time when held at high temperature (*4*) and loss of surface area goes hand in hand with loss of activity (*5*). Figure 5 shows the effect on both the alumina and free nickel surface areas of time and temperature when the catalyst was exposed to a 90:10 vol mixture of steam and hydrogen at 25 atm pressure (*4*). Loss of area is rapid during the first 100 hr and larger at higher temperatures but then settles out to a slow loss with time. Clearly the influence of this phenomenon on activity loss will be most marked at shorter times. This is illustrated

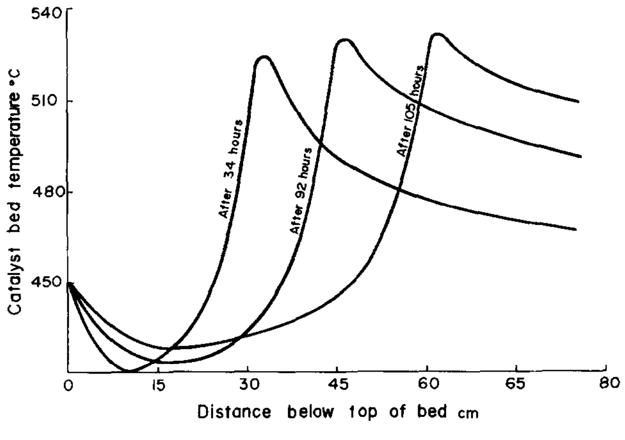

FIG. 4. Reaction temperature profiles with time through 0.44 cm i.d. catalyst bed: conditions as in Fig. 3.

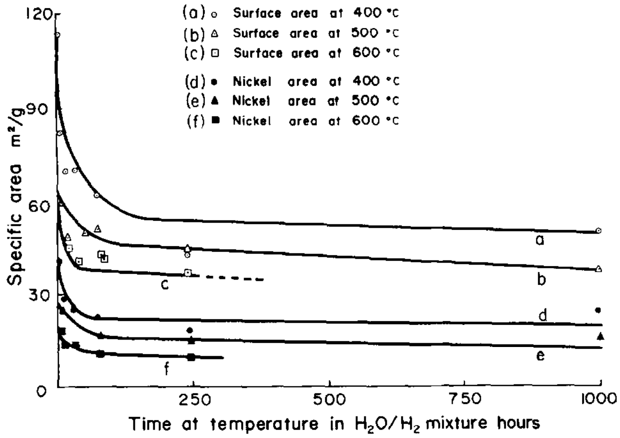

FIG. 5. Sintering of nickel-alumina catalyst in steam-hydrogen mixtures with time and temperature: steam-hydrogen volume ratio, 9:1; total pressure, 25 atm.

in Fig. 6 which shows the curves obtained in a 38 cm bed with initially unsintered catalyst and two other samples which were sintered at 500°C in a stream of equilibrium product gases supplied from another apparatus for 72 and 163 hr, respectively, before steam and distillate supply was commenced. After considerable divergence at short times, the curves tend towards similar slopes as the changes in areas with time due to sintering become small. Sintering also leads to some shrinkage of catalyst bed and this too will influence the progression curves somewhat in the early stages.

Thirdly there is the most important contribution to loss of activity, poisoning by a constituent or constituents of the feedstock. This rate of poisoning is strongly dependent on the final boiling point of the distillate supplied. Three distillates with final boiling points of 115, 140, and 170°C were supplied to the 38 cm reactor under otherwise identical conditions and gave the results of Fig. 7. The resistance to poisoning of the catalyst as expressed arbitrarily by the inverse slope of the curves at long times where sintering makes a very small contribution to activity loss changed from 8.7 kg of distillate pumped/g of catalyst deactivated for 115°C distillate to 5.0 kg/g for 140°C distillate and finally to 1.9 kg/g for the distillate with a final boiling point of 170°C. The higher boiling distillates have higher percentages of aromatics and higher molec-

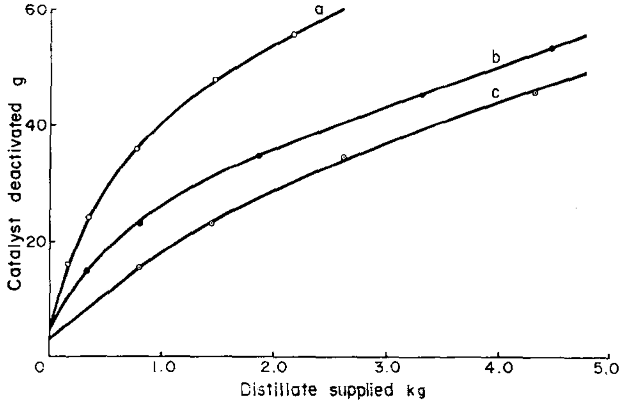

FIG. 6. Influence of pretreatment in product gases at 500°C on poisoning curves: catalyst bed 38 × 0.44 cm of 18–30 BSS particles in all cases; weight of charge, 6.0 g before reduction; other conditions as in Fig. 3; (a) ○, no pretreatment; (b) ●, 72 hr pretreatment; (c) ⊙, 163 hr pretreatment.

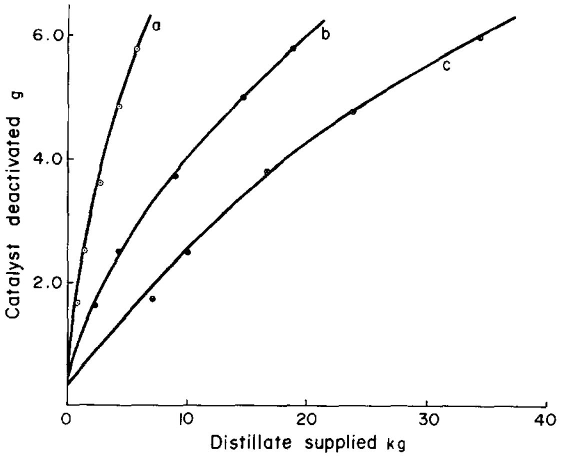

FIG. 7. Effect of distillate final boiling point on rate of poisoning: catalyst bed 38 × 0.44 cm of 18–30 BSS particles in all cases; weight of charge, 6.0 g before reduction; other conditions as in Fig. 3; (a) ⊙, 170°C FBP distillate; (b) ●, 140°C FBP distillate; (c) ⊕, 115°C FBP distillate.

ular weights (see Table 1). Tests made using small quantities of pure aromatic, cyclic, and paraffinic hydrocarbons dissolved in *n*-heptane as feedstock indicated that for hydrocarbons of about the same molecular weight, aromatics were most deleterious, cyclics next, and paraffins least, though generally differences were not marked. The xylenes, though not toluene and benzene, seemed particularly harmful. Increasing molecular weight increased the poisoning rate with both pure paraffins and pure cycloparaffins in line with the experiments with distillates of increasing boiling point.

TABLE 1
PROPERTIES OF LIQUID HYDROCARBON DISTILLATES

bp (°C)			Aromatics	
Initial	Mol av	Final	(wt %)	Mol wt
44	72	115	3.2	83
34	76	140	4.7	90
46	86	170	5.5	96

2. Space Velocity

The effects on catalyst life of changes in reactant mass flow rate at constant composition and operating conditions were examined in 38 and 84 cm beds. The initial reaction zone as represented by the temperature profile became twice as long and the rate of temperature rise with length in the exothermic stage of the reaction was halved when the total feed rate was doubled. The life of the catalyst as expressed by the final inverse slope of the poisoning curves (kg of distillate gasified/g of catalyst) was little effected by space velocity but did decrease very slightly at higher throughputs. The active life of the first few inches of bed was lower at higher throughputs, no doubt due to the longer temperature profile and the changed interaction between loss of area by sintering and poisoning in the longer reaction zone.

3. Temperature

Runs were made under standard conditions at 25 atm in 38 cm beds with the preheater and reactor temperatures set initially at 425, 450, and 475°C. In a system with no heat loss, the temperatures achieved at each stage of conversion depend on the total heat content of the gas, of which the preheat provides a fraction only. Thus for a 25°C rise in preheat temperature for example, the temperature rise on completion of the reaction is not 25°C. The minimum and maximum temperatures of the initial profile recorded for each preheat temperature are listed in Table 2, which shows that the minimum temperature was raised by some 17°C and the maximum by 15°C for

TABLE 2
EXPERIMENTS ON THE EFFECTS OF TEMPERATURE UPON POISONING
Maximum and minimum bed temperatures observed at various initial reactor temperatures.

Reactor and preheater temp (°C)	Temp of profile (°C)	
	Minimum	Maximum
425	395	510
450	412	525
475	438	540

each 25°C rise in preheat over this temperature range. Even though these temperature changes are not great, they have a marked effect on the poisoning curves illustrated in Fig. 8, with catalyst lives taken from the inverse final slopes of 4.2, 2.8, and 1.0 kg/g for nominal temperatures of 475, 450, and 425°C, respectively. No doubt the true decrease in distillate poisoning rate per active site with temperature increase is even greater, since it will be recalled that higher temperatures lead to enhanced sintering and a smaller residual stable surface area. Two experiments made in 84 cm beds at 470 and 450°C gave 4.2 and 2.7 kg/g, respectively, both larger values as was usual for the longer beds in which the progression curve can settle to a straight line, but confirming the effect of temperature.

All attempts at experiments at initial bed temperatures of 500°C with 18–30 BSS powders were terminated rapidly by blockage of the bed. When the reactor was dismantled considerable quantities of carbon were found on the catalyst at the entrance which were not in evidence at lower temperatures.

4. Pressure

Five experiments were made in the 84 cm reactor tube on 18–30 BSS catalyst particles at constant standard mass feed rates of water and 170°C distillate in the usual ratio of 1.66:1 by weight at five different total pressures: 9, 11, 14.75, 25, and 43 atm. In each case, the early temperature profiles were of approximately similar length, qualitatively indicating a zero order gasification reaction with respect to total pressure. Rises in pressure lead to rises in temperature at each stage of the distillate conversion, since the production of methane which is exothermic involves a decrease in the number of molecules. At feed temperatures of 450°C, the temperature changes are not great, the minimum temperatures recorded in the bed being 419, 421, 426, 424, and 429°C at 9, 11, 14.75, 25, and 43 atm, with corresponding maxima of 526, 526, 526, 530, 530, and 531°C. The results are illustrated in Fig. 9, which shows that the final rate of progression through the bed is roughly independent of pressure, though there is a tendency for the catalyst in the experiments at lower pressures to be poisoned more quickly in the early stages leading to a displacement of one curve from

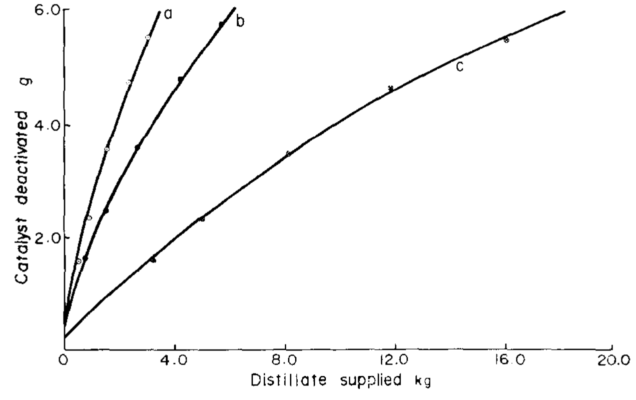

FIG. 8. Effect of temperature on rate of poisoning: catalyst bed 38 × 0.44 cm of 18–30 BSS particles in all cases; weight of charge, 6.0 g before reduction; other conditions except temperature as in Fig. 3; steam: distillate inlet and initial bed temperature: (a) ⊙, 425°C; (b) ●, 450°C; (c) ⊕, 475°C.

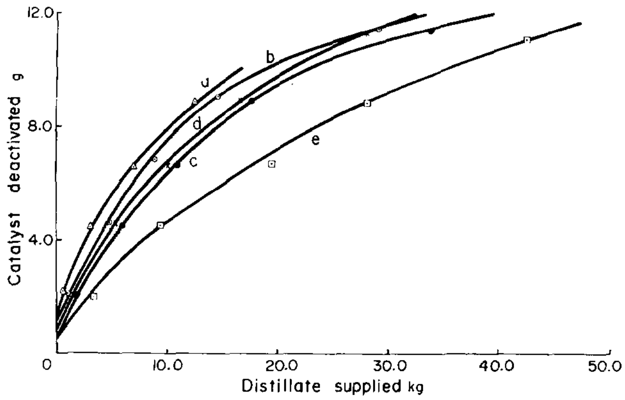

FIG. 9. Effect of pressure on rate of poisoning: conditions as in Fig. 3 except pressure; (a) △, 9.0 atm; (b) ⊙, 11.0 atm; (c) ●, 14.75 atm; (d) ×, 25 atm; (e) ⊡, 43.0 atm.

another which persists throughout the experiments. Bearing in mind the slightly lower average temperatures at lower operating pressures and that lower temperature tends to enhance poisoning, the experiments at lower pressures may have a rather smaller poisoning rate after long times, but clearly the influence of total pressure on poisoning is not great.

5. *Steam Hydrocarbon Ratio*

A series of nine experiments were made in 84 cm beds of 18–30 BSS catalyst with a constant hydrocarbon mass feed rate of 39 g/hr, in which the water feed rate was varied to examine the effect on poisoning of changing the steam:distillate ratio. Total pressure was constant in seven experiments at 25 atm. In two experiments, changes in pressure were made to such an extent as to maintain the hydrocarbon partial pressure at its normal value at three steam:distillate ratios. Table 3 sets out the conditions for these experiments, shows the approximate resistance to poisoning of the catalyst in each case as determined from the inverse slope of the final progression curve, and, by quoting the minimum and maximum temperatures observed by the thermocouples 15 and 60 cm from the bed entrance, indicates the effect of changing steam:distillate ratio on the uncontrolled variable of temperature. As shown, increased steam:distillate ratio at constant total pressure leads to a

TABLE 3

CONDITIONS USED, MAXIMUM AND MINIMUM TEMPERATURES OBSERVED AND CATALYST RESISTANCE TO POISONING MEASURED IN EXPERIMENTS AT VARIOUS STEAM:HYDROCARBON RATIOS

Run No.	Feed wt ratio H_2O/HC	Feed molar ratio H_2O/HC	Total pressure (atm)	Partial pressure (atm)		Recorded temp (°C)				Resistance to poisoning (kg/g)
				Hydrocarbon	Steam	Minimum		Maximum		
						15 cm point	60 cm point	15 cm point	60 cm point	
9/112	1.2	6.7	25.0	3.3	21.7	440	440	530	531	2.2
8/191	1.66	9.2	25.0	2.4	22.6	426	450	514	529	2.9
8/181	1.66	9.2	25.0	2.4	22.6	422	448	520	530	2.9
9/87	1.66	9.2	25.0	2.4	22.6	420	450	519	540	2.9
4/93	2.0	11.1	25.0	2.1	22.9	420	445	504	528	3.8
9/102	2.0	11.1	29.5	2.4	27.1	410	434	500	516	3.8
9/100	3.0	16.7	25.0	1.4	23.6	412	430	482	509	5.0
9/101	3.0	16.7	43.0	2.4	40.6	413	449	488	519	5.0
9/103	5.0	27.8	25.0	0.9	24.1	400	409	452	477	6.3

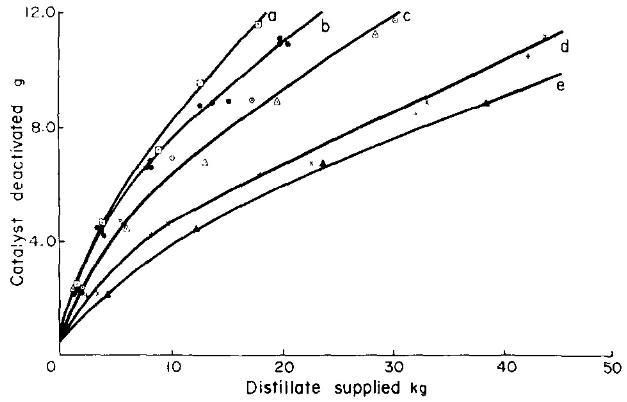

FIG. 10. Effect of steam hydrocarbon feed ratio on rate of poisoning: catalyst charge and temperature as in Fig. 3; distillate feed rate, 39 g/hr; water feed rate variable; water:distillate feed weight ratio: (a) ⊡, 1.20, pressure, 25 atm; (b) ●, 1.66, 25 atm; 3 experiments; (c) ⊙, 2.0, 25 atm. △, 2.0, 29.5 atm; (d) +, 3.0, 25 atm. ×, 3.0, 43.0 atm; (e) △, 5.0, 25 atm.

lowering of the temperature of reaction at all stages of conversion, which is in line with theoretical predictions assuming product equilibrium since increased unreacted steam will suppress the exothermic methane synthesis reaction at each stage of distillate decomposition. The poisoning curves are illustrated in Fig. 10. As might be expected from the results of Sect. 4 above, changes in total pressure at constant steam hydrocarbon ratio had little effect, but decreasing the ratio led to a rapid decrease in the resistance of the catalyst to poisoning. Furthermore, the true improvements in resistance at high steam distillate ratios will be bigger than those indicated by Fig. 10 or the last column of Table 3, since the overall reaction temperature is lower, particularly at higher ratios, and lower temperatures favor more rapid poisoning.

6. Particle Size

Experiments were made in 38 cm tubes with 170°C final boiling point distillate at 25 atm, 1.66:1 steam:hydrocarbon ratio and standard conditions to establish the effect of catalyst particle size on activity loss. Particle size ranges of 36–52, 18–30,

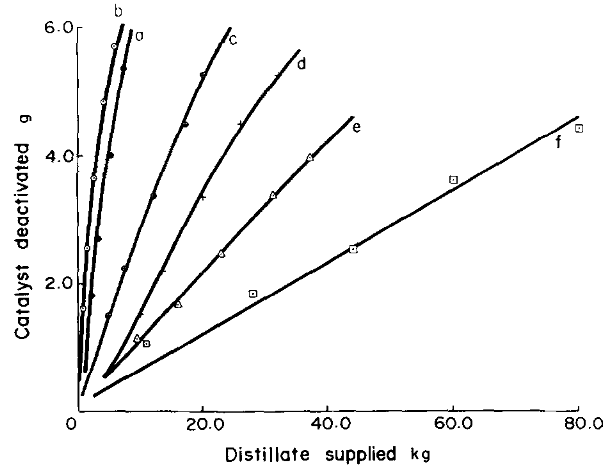

FIG. 11. Effect of particle diameter on rate of poisoning: catalyst bed 38 × 0.44 cm; other conditions except particle size as in Fig. 3; (a) ●, 36–52 BSS particle size; (b) ⊙, 18–30 BSS; (c) ⊕, 10–14 BSS; (d) +, 8–10 BSS; (e) △, 6–8 BSS; (f) ⊡, 0.32 cm equant cylinders.

TABLE 4
VARIATION OF LENGTH OF REACTION ZONE FROM 450°C TO THE MAXIMUM WITH PARTICLE DIAMETER AS SHOWN BY THE TEMPERATURE PROFILES

Particle size (BSS)	Arithmetic av particle diam (cm)	Zone length (cm)
36–52	0.036	6.3
18–30	0.067	6.3
10–14	0.145	7.5
8–10	0.187	10.0
6–8	0.244	13.0
0.32 cm cylinders	0.320	19.0

10–14, 8–10, 6–8 BSS and 0.32 cm equant cylindrical pellets were used. The results are illustrated in Fig. 11. At first increasing particle size had little effect (compare 36–52 and 18–30 mesh, the displacement in the curves is probably due to shrinkage), but thereafter there was a rapid increase in resistance to poisoning. The reaction zone increased markedly in length with particle size above 10–14 BSS (see Table 4) until it became roughly proportional to the pellet diameter, indicating the onset of diffusional control of the reaction rate. The poisoning plots of Fig. 11 still showed considerable curvature and the reaction zone was an appreciable fraction of the whole bed length with larger particles. The experiments were therefore repeated in 84 cm beds for 18–30 BSS powder and 0.32 cm pellets, and gave the results shown in Fig. 12. The resistance to poisoning of the 0.32 cm pellets as measured by the slope of the final progression curve was 15 kg/g, or about 6 times that of the 18–30 BSS powder. Larger diameter cylinders could not be used in the laboratory but tests were made using 0.32, 0.64, and 0.80 cm cylindrical pellets on a small pilot plant with a reaction tube 5 cm i.d. by 180 cm long, fitted with a movable thermocouple in a small sheath tube passing through the center of the reactor. These showed that resistance to poisoning was improved some 55% by using 0.64 cm cylinders instead of 0.32 cm but 0.80 cm cylinders showed little further improvement. The reaction zone length in these experiments was exactly proportional to the pellet diameter indicating complete diffusional control of the reaction rate. These data taken together indicate that the improvement in resistance to poisoning is associated with the transition region from chemical to diffusional control of the reaction rate.

The pilot plant data obtained with cylindrical pellets also revealed another interesting phenomenon. In many cases the endothermic low temperature region at the front of the reaction zone was almost absent in the early stages of the experiments and only began to develop properly after many

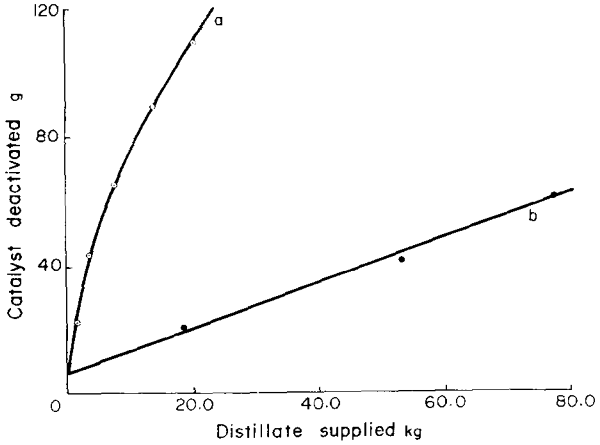

FIG. 12. Effect of particle diameter on rate of poisoning in long beds: catalyst bed 84 × 0.44 cm as in Fig. 3 and similarly for the other conditions except particle size; (a) ⊙, 18–30 BSS particle size; (b) ●, 0.32 cm equant cylindrical pellets.

hundreds of hours of operation, becoming progressively deeper.

The experiments in the laboratory showed similar effects, although the smaller scale of operation and closeness of the surrounding furnace held at 450°C naturally meant laboratory reactors were not as adiabatic as the large plant. Figure 4 shows the shape of temperature profiles over a range of times during the poisoning of 18–30 BSS catalyst under standard laboratory conditions; and Fig. 13 shows the same profiles when using 0.32 cm equant cylinders. Reference to Fig. 4 or Fig. 13 shows that operation is not adiabatic since the temperature falls from a maximum going down the bed as heat loss to the reactor at 450°C occurs after reaction is completed. The heat loss is actually worse than indicated by the temperature fall because the loss takes place in the presence of catalyst, the gaseous equilibria readjust, further methane is synthesized and this reaction liberates heat. No significant fall in temperature was observed in the more adiabatic pilot scale reactors after completion of the gasification. Nonadiabatic operation on the small scale also shows up in the tendency of both the minimum and maximum temperatures of the reaction zone in Figs. 4 and 13 to rise with progression of the zone through the bed. This is because the endothermic region with temperatures below 450°C lengthens, and heat is transferred from the furnace to the reacting gases on an increasing scale.

Comparison between Figs. 4 and 13 shows that the minimum temperatures observed were lower and the maximum temperatures higher for beds of 18–30 mesh particles than for beds of 0.32 cm pellets, even though all other conditions were the same. The profiles for the experiments with the other particle sizes confirmed this observation and revealed a progressive rise in minimum and fall in maximum observed temperature as particle size increased.

The fall in maximum temperature with increasing particle size in the laboratory tests is most probably a consequence of heat transfer, since the reaction zone at temperatures in excess of 450°C in front of the maximum is longer with bigger particles and heat loss will therefore increase in this region. This is supported by the more adiabatic pilot plant tests where the *maximum* temperature reached was independent of particle size. In any case without heat loss in an infinite bed the products must reach equilibrium and therefore the exit temperature must be constant for constant reactor conditions and independent of the form of the catalyst.

This explanation will not serve for the changes in minimum temperature. As Figs. 4 and 13 show, the minimum temperatures recorded by the 15 cm thermocouple for example, were approximately 423 and 440°C for 18–30 mesh powder and 0.32 cm pellets, respectively. Up to this point the bed will be colder than 450°C so the reactants will gain heat and since the mini-

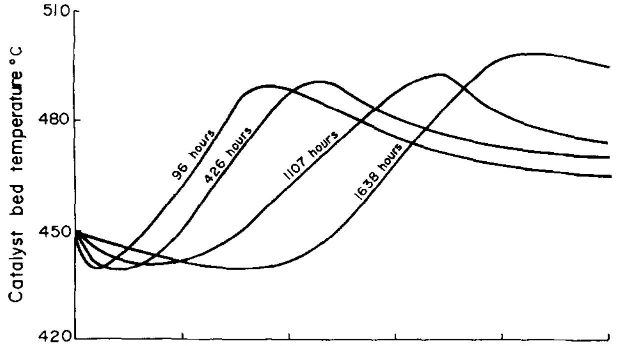

Fig. 13. Reaction temperature profiles with time through an 0.44 cm i.d. catalyst bed packed with 0.32 cm equant cylindrical pellets: conditions other than particle size as in Fig. 4.

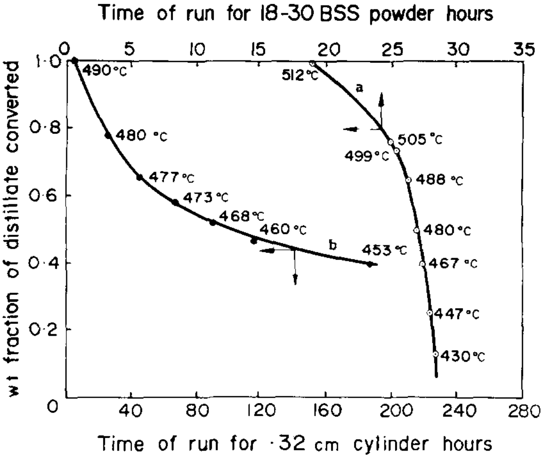

FIG. 14. Hydrocarbon slip through deactivating 12.5 cm beds of catalyst: pressures, feed rates, and inlet temperatures as in Fig. 3; bed length, 12.5 cm; (a) ⊙, 18–30 BSS powder; (b) ●, 0.32 cm equant cylindrical pellets. The bed exit temperature recorded when each sample was taken is shown on the curves in each case.

mum is lower with the smaller particles, the reactants will gain more heat in the same length of tube in this case.

The difference in minimum temperatures observed with pellets and powders could only mean that the product gases at the same low distillate conversion were not at equilibrium and that more methane must be present over the pellets, since the formation of methane is exothermic and the pellets showed the higher minimum temperature.

This was confirmed experimentally in the laboratory by packing two reactors with 13.5 cm beds of 0.32 cm equant cylinders and 18–30 BSS particles, respectively; the remaining space in each case being filled with inert α-alumina cylinders or particles with thermocouples located at the catalyst/alumina interfaces. Operating at 25 atm, 450°C, and 1.66 steam:hydrocarbon weight ratio, observations were made of the hydrocarbon ungasified, its increase with time, the exit temperature from the catalyst, and the dry product gas analysis and production rate. Figure 14 shows the fall in fraction of distillate gasified with time for the two experiments. As expected, the loss of activity as measured by the extent of gasification is much more rapid on the 18–30 mesh catalyst but little can be deduced from the curves beyond this because their shape is a complex function of the kinetics of the poisoning and gasification reactions and of a changing bed temperature which will certainly change both poisoning and gasification rates. The measured dry product gas analyses at various hydrocarbon conversions are set out in Table 5, together with the exit temperatures from the beds. Also shown are the gas compositions to be expected at each exit temperature and conversion calculated by means of a computer program which assumed equilibrium and that undecomposed hydrocarbons other than methane behaved as inert gases. As shown by Table 5, at hydrocarbon conver-

TABLE 5

METHANE DEFFICIENCY AND HYDROGEN EXCESS COMPARED TO EQUILIBRIUM AT PAR

Particle size (cm or BSS)	0.32		18–30		0.32		18–30	
Bed exit temperature (°C)	453		475		444		431	
Fraction of hydrocarbon unconverted (%)	59.9		59.7		74.0		74.4	
Exit gas analysis,	(a)[a]	(b)	(a)	(b)	(a)	(b)	(a)	(b)
(vol %, dry basis)	450°C		475°C		445°C		430°C	
CO_2	22.76	22.91	22.10	22.90	22.54	23.07	23.11	23.04
H_2	23.13	19.82	27.43	23.03	29.80	25.32	31.10	23.58
CO	0.35	0.29	0.51	0.42	0.32	0.22	0.30	0.17
CH_4	52.85	56.96	48.02	53.65	47.03	50.38	45.04	53.20
N_2	0.8	—	0.6	—	0.30	—	0.45	—
Equiv temp (°C)								
$(CO_2)(H_2)/(CO)(H_2O)$	453	450	468	475	459	445	445	430
$(CO)(H_2)^3/(CH_4)(H_2O)$	470	450	492	475	460	445	466	430
$(CO_2)(H_2)^4/(CH_4)(H_2O)^2$	467	450	496	475	460	445	466	430

[a] (a) Measured; (b) calculated, assuming equilibrium at the temperature shown.

sions above 40%, equilibrium is approached over both catalysts. As conversion decreases and bed exit temperature falls, observed hydrogen (and carbon monoxide) rises above the equilibrium value and methane falls below it for the 18–30 BSS particles but there is little change from equilibrium for the pellets. The considerable excess of hydrogen noted in the early stages of the reaction on 18–30 BSS powder is in agreement with earlier kinetic studies of the gasification (*2*).

Discussion

1. *The Shape of the Temperature Profiles*

The shape of the temperature profiles merits some consideration. The initial S-shaped profile is upright but during the first few hours of operation as well as progressing through the bed, it tends to flatten and lengthen, i.e., the exothermic temperature profile decreases in gradient. Thereafter, when the initial rapid sintering of the whole bed is over, the progression through the bed continues over hundreds of hours but the exothermic profile maintains its slope throughout. Some residual activity remains at the front of the bed, since the temperature in this region is still below the gas inlet temperature, and this activity persists for a very long time. That is to say the front end of the reaction zone at temperatures below the inlet temperature continuously extends and changes shape with time, but the exothermic region does not change its shape though it does move forward through the bed. These phenomena seem at first sight to indicate two things.

First, sintering, which affects the whole bed and would therefore cause the whole zone to increase in length, makes a negligible contribution to the loss of activity after the initial stages.

Second, little poisoning of the catalyst occurs towards the exit end of the reaction zone and progression occurs as a result of poisoning at the entrance of the zone in the low temperature region. This observation seems scarcely surprising since it is in accord with the results which show improved life at higher temperatures and higher steam:distillate ratios (as gasification proceeds the steam:distillate ratio rises, steam being present in large excess). Furthermore, although this effect must be small, there is evidence that at equal partial pressures higher hydrocarbons are adsorbed on the catalyst surface slightly more preferentially (*2*) and higher hydrocarbons certainly poison more rapidly as shown by the effect of distillate boiling point on catalyst life. The catalyst surface at the front of the zone will adsorb and gasify slightly more of the higher hydrocarbons than the surface at the exit where the ungasified distillate will contain fractionally more light ends. (Preferential gasification

TIAL FEEDSTOCK CONVERSIONS ON 18–30 BSS POWDERS AND 0.32 cm EQUANT CYLINDERS

0.32		18–30		0.32		18–30		0.32		18–30	
441		420		439		414		438		418	
85.0		86.2		89.8		90.8		95.0		94.9	
(a)	(b)	(a)	(b)	(a)	(b)	(a)	(b)	(a)	(b)	(a)	(b)
440°C		420°C		440°C		415°C		440°C		420°C	
21.49	23.34	22.81	23.28	21.65	23.53	21.86	23.45	21.14	23.84	22.16	23.81
37.65	34.45	49.16	30.13	42.62	42.55	70.75	36.92	56.85	56.32	72.62	53.13
0.19	0.19	0.28	0.13	0.14	0.17	0.32	0.11	0.16	0.15	0.27	0.10
39.78	42.12	27.48	46.46	34.88	33.74	6.47	39.52	21.37	19.66	4.36	23.95
0.79	—	0.25	—	0.70	—	0.60	—	0.48	—	0.60	—
439	440	430	420	430	440	422	415	445	440	425	420
440	440	482	420	432	440	535	415	434	440	525	420
440	440	492	420	435	440	558	415	430	440	545	420

of heptane in a partially converted heptane–hexane mixture was observed in carefully controlled laboratory experiments on pure hydrocarbons (*2*) but, somewhat surprisingly, no change in composition between ungasified product distillate and feedstock could be detected by chromatographic methods when complex distillates were supplied to a catalyst bed which was not long enough to complete the gasification. The effect of preferential adsorption of higher hydrocarbons at the front of the reaction zone cannot therefore be large.)

There is no doubt about the first point: the curve shapes show that sintering is not a major contributor to poisoning after the early stages. However, the second point, though plausible, cannot be proved by reference to the shape of the temperature profile alone. Regardless of preferential frontal poisoning, it seems to be a characteristic property of all catalyst beds in which the bed is long compared to the reaction zone and which are poisoned by interaction with the feed that the zone moves forward in this way, essentially because fresh unpoisoned catalyst is continually being introduced and utilized at the exit end of the zone.

2. The Reaction on Powdered Catalyst

In previous papers (*2, 6*), the rate of gasification of light hydrocarbons with steam over powdered catalyst was shown to be zero order with respect to steam and very close to zero order with respect to hydrocarbon, at hydrocarbon partial pressures down to 0.25 atm and at distillate conversions of up to at least 70%. The activation energy of the overall gasification was about 20 kcal/mole. When 0.32 cm pellets were used, the order with respect to hydrocarbon rose to slightly greater than one half and the activation energy fell to 10 kcal/mole, indicating diffusional limitation of the rate for larger particles. It was further shown that, over powdered catalysts, hydrogen and carbon monoxide were produced in quantities in excess of equilibrium at low conversions but that, as conversion progressed, the excess disappeared and this indicated that hydrogen and carbon monoxide were the primary products of the reaction and the synthesis of methane from them was rather slower than the rate of the hydrocarbon gasification. No work was reported in these papers on loss of catalyst activity.

The form of the poisoning curve observed with powders in this paper arises from the complex interplay of two factors.

Clearly the results indicate that the catalyst is poisoned by the distillate, more rapidly by higher boiling compounds (Fig. 7), and generally by all hydrocarbon structures, though some are worse than others. Thus any hydrocarbon molecule which gasifies can also poison and this implies that the poisoning reaction proceeds in parallel with the gasification reaction, though obviously at a much lower rate since large quantities of hydrocarbon can be gasified by a small quantity of catalyst before it becomes inactive. The fact that distillate boiling point has such a large effect on the poisoning of the catalyst indicates that the composition of the product gases *does not* have a significant influence on the poisoning reaction at normal operating temperatures.

Independently, activity loss occurs through loss of surface area by sintering and the rate of this process is time and temperature dependent (Fig. 5). After a comparatively short time, further loss of area by sintering (to which the whole bed is exposed from start-up) is slow and therefore the rate of poisoning after a long time (i.e., after a reasonable depth of bed has been deactivated) is mainly caused by the hydrocarbon feedstock. Qualitatively, bearing in mind the system is not isothermal, the results in this region show that the rate of progression of the reaction zone through the bed is: (a) Lower at higher temperatures over a narrow temperature range around 450°C (Fig. 8). (b) Approximately independent of total pressure (Fig. 9). (c) Roughly proportional to distillate steam ratio in the feed (Fig. 10), after allowance for temperature effects. (d) Nearly independent of rate of feedstock supply, when expressed as grams of catalyst per kilogram of distillate gasified.

Any mechanism proposed for the reactions taking place must explain these gross properties shown by the progression curves through the bed. Unfortunately, apart from this, the detailed shape of the curves, even if it were available free of sintering and variable temperature effects, is very insensitive to the kinetic order chosen for the poisoning reaction and the relationship between extent of poisoning and residual activity, and can throw little light on either of these.

Bearing in mind that the gasification reaction is zero order, which implies complete occupation of active sites, the simplest possible sequence of reaction steps to explain these gross properties would be:

$$\begin{array}{llll} C_nH_{2n+2} & \rightarrow S_1 & K_1 & (3) \\ S_1 & \rightarrow S_2 & K_g & (4) \\ S_2 + H_2O & \rightarrow \text{Products} & K_w & (5) \\ S_2 + C_nH_{2n+2} & \text{Poison or poison precursor} & K_p & (6) \end{array}$$

Where C_nH_{2n+2} and H_2O are the gaseous concentrations of steam and hydrocarbon, respectively, and S_1 and S_2 are absorbed hydrocarbon species. If $K_1(C_nH_{2n+2}) \gg K_g < K_w(H_2O) \gg K_p(C_nH_{2n+2})$, then the initial rate of gasification is zero order with respect to steam and distillate and is given by K_g. The stationary concentration of S_2 is:

$$(S_2) = K_g/K_w(H_2O)$$

and the initial rate of poisoning is given by:

$$dp/dt = K_gK_p[(C_nH_{2n+2})/K_w(H_2O)].$$

Reaction (6) between a surface species and gaseous hydrocarbon seems a little unlikely, but a reaction of this type must occur to provide the observed dependence of poisoning on steam distillate ratio.

Before turning to consider the progression curve in more detail it is worth noting two points. First, the surface transition $S_1 \rightarrow S_2$, the postulated rate controlling gasification reaction (4), may involve a series of steps, since previous work (*6*) on this catalyst with hexane *or* heptane has shown that their rates of gasification are identical when expressed as grams of carbon gasified per unit time per active site. This indicates that the rate controlling step is the reaction on each surface site of identical species (perhaps for example CH_2) whatever the starting hydrocarbon provided it is straight chain (branch chain hydrocarbons and aromatics had differing rates to straight chain hydrocarbons) whereas S_1 in this simple scheme is likely to be different for different hydrocarbons. Second, reaction (6) must be a simplification because some experiments showed that if hydrocarbon supplied to the bed were cut off for a time not too long after the beginning of the test and then restarted, some reactivation of poisoned sites by steam alone took place, but this reactivation was much less if the bed had been gasifying for a long time. Clearly this implies that poison can be removed slowly by steam in the same way as S_2 provided it has not been on the surface too long. The poison appears to "toughen" on the surface with time, perhaps by dehydrogenation and polymerization.

A more detailed mechanism taking these facts into account with approximately similar overall consequences would be:

$$\begin{array}{lll} C_nH_{2n+2} & \rightarrow S_1 & \text{Fast} \\ S_1 & \rightarrow S_2 & \text{Fast} \\ S_2 & \rightarrow S_3 & K_g \text{ (slow)} \\ S_3 + H_2O & \rightarrow \text{Products} & K_{w1} \\ S_3 + C_nH_{2n+2} & \rightarrow S_4 \text{ (poison which can be removed slowly by steam)} & K_{p1} \\ S_4 + H_2O & \rightarrow \text{Products} & K_{w2} \\ S_4 + C_nH_{2n+2} & \rightarrow \text{More firmly held poison} & K_{p2} \end{array}$$

with S_2 the same species for all hydrocarbons. As poisoning progresses and consumes active sites, the rate of gasification per unit weight of catalyst will fall and this gives rise to the progression curves in the following way.

The relationship between residual activity and extent of poisoning is not known. The simplest assumption that can be made is that activity falls linearly with poisoning; that is if there are N_0 sites per unit area initially and p sites are poisoned after time t, the residual activity is $(N_0 - p)$. The rate of gasification, originally N_0K_g per unit area for zero order reaction if K_g is the rate constant per site, will be $K_g(N_0 - p)$ at time t, if the gasification rate is proportional to the number of free sites. This is supported by the fact that gasification activity is very approximately proportional to the measured remaining nickel surface area on poisoned catalysts (*5*). Thus (S_2) at time t in the simple scheme will be given by:

$$(S_2) = K_g(N_0 - p)/K_w(H_2O), \qquad (7)$$

in the instantaneous steady state which will apply because poisoning is much slower than gasification and the rate of poisoning by:

$$dp/dt = [K_g K_p(C_nH_{2n+2})(N_0 - p)]/K_w(H_2O). \qquad (8)$$

Integrating Eq. (8) with $p = 0$ when $t = 0$ gives:

$$(N_0 - p)/N_0 = \exp\{[-K_g K_p(C_nH_{2n+2})t]/K_w(H_2O)\} \qquad (9)$$

where $(N_0 - p)/N_0$ is the fraction of the original sites or activity remaining after time t.

Suppose $N_0{}^1$ sites are required to complete the reaction and these are available in length L_0 of unpoisoned catalyst bed. The original bed length to complete the reaction will be L_0 and the reaction zone will spread to fresh unpoisoned catalyst as poisoning occurs in L_0 so that after time Δt, the new length $L_0 + \Delta L$ still contains $N_0{}^1$ sites. This progression can be summed over successively small increments of time with activity loss according to Eq. (9), assuming the distillate:steam ratio remains constant during reaction (a considerable approximation except at low conversions) and the result is the straight-line progression through the bed with poisoning time given by:

Length at time

$$t = L_0 + L_0 t \times \left[1 - \exp\left(\frac{-K_g K_p(C_nH_{2n+2})}{K_w(H_2O)}\right)\right]$$

with intercept L_0 at zero time, or, when K_p is very small and poisoning is a slow reaction:

$$L_t = L_0 + \{[L_0 K_g K_p(C_nH_{2n+2})t]/K_w(H_2O)\}.$$

Then the slope of the progression curve through the bed with time is proportional to the hydrocarbon:steam ratio in the feedstock and independent of total pressure. The L_0 is inversely proportional to K_g so that the rate of progression through the bed or poisoning will fall with increasing temperature as indicated by the experimental results, if the activation energy of the poisoning reaction (E_p) is less than that for the reaction of steam with species S_2 (E_w). The changes in poisoning rate with temperature shown in Fig. 8 indicate that the negative activation energy associated with the rate constant ratio K_p/K_w is between 60 and 70 kcal/mole. Thus even if E_p were 0, $E_w >$ 60 kcal/mole.

It is noticeable that the experimental progression plots show a curvature even when the bulk of simple sintering and shrinkage has been eliminated by complete treatment in product gases (see Fig. 6) and the curvature persists up to several times the original bed length whereas exponential loss of active sites with time indicates a straight line. Other poisoning mechanisms are possible and give the gross properties observed, provided competing reactions of the same order with respect to distillate and steam are retained. Some of these mechanisms give curves in the early stages, but all become straight before the experimental plots.

It is likely that the curvature is a consequence of the only partially adiabatic conditions in the laboratory experiments. After the main reaction zone has passed by, the temperature of the catalyst which retains a residuum of activity, begins to rise from the endothermic minimum back towards the reactor temperature and the maximum temperature also rises (Fig. 4). The poisoning rate will fall compared with the gasification as the average bed temperature rises and this will cause the rate of progress of the zone through the bed to diminish somewhat. This is supported by pilot plant data from experiments using 0.32 cm pellets (*3*). Here the progression through the bed is linear with time after the initial sintering but as has been explained the endothermic dip is largely absent so that temperatures in front of the main reaction zone are more nearly constant and close to the preheat temperature; and the maximum temperature is constant too.

It might appear from the results and from the discussion that low temperature oil gasification catalysts of the type described would give more satisfactory resistance to poisoning if operated at higher temperatures but this is not so. It will be recalled that experiments with 18–30 BSS powders at starting temperatures of 500°C and more blocked rapidly with carbon and could not be completed. There may be several reasons for this: (i) The higher the temperature of operation, the greater the initially rapid and subsequently gradual loss of catalyst surface area with time due to sintering, which can become the limiting factor especially with deep beds and slower poisoning lighter hydrocarbons even though the rate of the gasification reaction per site rises with temperature. (ii) At constant distillate:steam ratio and pressure, higher temperatures given more carbon monoxide and less carbon dioxide in the product gases so that the point at which carbon is deposited on the nickel surface by the equilibrium $2CO = CO_2 + C$ is more closely approached. (iii) Another poisoning reaction such as the simple pyrolysis of hydrocarbons to carbon may begin to take place at a significant rate at higher temperatures.

3. The Effects of Particle Size

The length of the initial reaction zone is independent of particle size for small particles; but, as the size increases, the length becomes proportional to the particle diameter, which is as expected if the gasification reaction passes from the regime of chemical control of rate to that of diffusional control. In line with this (*2*, *6*), the activation energy of the gasification reaction falls from 20 to 10 kcal/mole and the order of the reaction with respect to hydrocarbon partial pressure rises from just over zero to just over 0.5 (*7*). The diffusional barrier occurs in the pores of the catalyst and the rate is not limited by mass transfer to the surface of the particles. The evidence for this is that 10 kcal/mole is too high an activation energy for a mass transfer process, and that the rate of gasification would not fall at all with poisoning if it were controlled by mass transfer.

The rate of the zero-order gasification reaction is K_gN_0 molecules per square centimeter of active area per second for small catalyst particles with no diffusional hindrance; whereas for large pellets it is proportional to $(rK_gN_0DC_0)^{1/2}/L$, where r is the pore radius, C_0 the hydrocarbon concentration at the pore entrance, D the diffusion coefficient and L the particle diameter (*7*). The overall order of reaction with respect to pressure on large particles (as opposed to the order with respect to hydrocarbon alone) will depend on whether D is the coefficient of Knudsen diffusion which is independent of pressure (overall order then 0.5) or the coefficient of bulk diffusion which is inversely proportional to pressure (overall order then zero) and the overall order has not been determined experimentally. Which diffusion coefficient controls the rate depends on whether the limitation on rate occurs within the macropore or micropore structure of the catalyst particle or a combination of both. The fresh catalyst has a number of macropores with diameters around 1000 Å and a further large number of micropores with diameters of 20–30 Å (*4*). Bulk diffusion will certainly operate in the larger pores; in the smaller, calculation shows that at 25 atm diffusion of the hydrocarbon steam mixture is in the transition region, which means that diffusion will be Knudsen at lower pressures but bulk at higher. Thus, if rate control occurs in the micropores, the overall order will fall from 0.5 to zero at typical operating pressures as these are raised.

The initial increase in resistance to poisoning with increasing particle diameter observed in this study is a surprising phenomenon; indeed the reverse behavior is customary in many catalytic processes (*8*). Clearly the improvement is associated with an increasing diffusional barrier but only to a point, because large increases in particle diameter do not continue the improvement, though the barrier continues to increase since the rate still falls off as the inverse of the diameter. Consideration of reactant concentrations within the pore can explain this behavior.

For a zero-order gasification reaction in pores (which will be the reaction that determines the concentration of hydrocarbon, since hydrocarbon disappearing by reaction to form poison is small) the concentration gradient in hydrocarbon down a pore is given by (7):

$$\frac{C_a}{C_0} = 1 - h^2\left[\frac{x}{L} - \frac{1}{2}\left(\frac{x}{L}\right)^2\right],$$

where $h = L(2K_gN_0/rDC_0)^{1/2}$,

and r is the pore radius, D the diffusion coefficient, x the distance from the entrance inside the pore, L the pore length (proportional to the particle diameter), C_0 the hydrocarbon concentration at the pore entrance in the main gas stream and C_a the concentration at penetration x.

If h is less than $\sqrt{2}$ because the particles are small or the concentration C_0 is high, C_a is greater than zero when $x = L$ and the zero order gasification reaction proceeds at full rate proportional to K_gN_0 and independent of the particle size, since all active catalyst surface has a finite hydrocarbon concentration above it. Even in this regime some improvement in catalyst life can be expected, since the rate of poisoning depends on the hydrocarbon steam ratio and for C_a less than C_0, the average value of the ratio down the pore will be lower than at the pore entrance, bearing in mind that although steam is consumed in gasification it is present in large excess to begin with at typical feed ratios and much remains when $C_a = 0$. In due course $h = \sqrt{2}$, either as a result of increasing pellet size or fall in C_0 as reaction proceeds through the bed. Here $C_a = 0$ at $x = L$ and a minimum in the average value of hydrocarbon:steam ratio per unit of exposed active surface is realized. This minimum per unit of exposed active surface is subsequently maintained with increasing diameter although less and less surface in each pore supports gasification, for when h is greater than $\sqrt{2}$, C_a falls to zero before $x = L$ according to a different equation (7):

$$\frac{C_a}{C_0} = 1 - 2\left[\frac{hx}{\sqrt{2}L} - \frac{1}{2}\left(\frac{hx}{\sqrt{2}L}\right)^2\right],$$

and $C_a = 0$ when $x = \sqrt{2}L/h$.

In this case only the length of pore given by $\sqrt{2}/h$ is gasifying and can be poisoned and the gasification rate becomes inversely proportional to L (or the particle diameter), though of course the gasification rate per unit surface area of catalyst exposed to hydrocarbon is unchanged. The catalyst at the bottom of the pore sees no hydrocarbon until that towards the entrance has lost some activity.

The average minimum value of C_a is readily calculated. The average concentration of hydrocarbon over the catalyst which is gasifying to pore depth x_m for all x up to $x = L$ is:

$$\frac{1}{x_m}\int_0^{x_m} C_a dx$$

with $x_m = \sqrt{2}L/h$ which has the value ⅓ C_0 where C_0, as before, is the concentration at the pore mouth. If the hydrocarbon: steam weight ratio initially were 1:1.66, the usual operating condition, and the average distillate concentration were down to ⅓ C_0, the ratio would fall to a minimum average of around 1:3.0 allowing for steam consumption by reaction.

Summarizing these conclusions for actual operation in a bed of catalyst supporting reaction, C_0 falls from its inlet value to zero as reaction proceeds. Thus, as the particle size of the bed is increased, diffusional effects first show at the exit end of the reaction zone. Though the reaction zone does not lengthen unless C_0 or L are such that h is greater than $\sqrt{2}$, there will be some improvement in resistance to poisoning since the average hydrocarbon:steam ratio will be lower for moderate sized than for small particles in this exit region. As the size and thus L is increased further, the reaction zone begins to lengthen and the average hydrocarbon:steam ratio falls over more catalyst.

Ultimately the particle size becomes big enough for the hydrocarbon concentration to fall to zero before the ends of the pores even at the reaction zone entrance where C_0 is at its maximum, the reaction rate becomes exactly proportional to particle diameter and the resistance to poisoning increases no further since C_a (av) is at its minimum of $\frac{1}{3}$ C_0 even at the zone entrance. As the results show, this is the type of behavior observed.

By the nature of the processes discussed above, preferential poisoning at the pore mouth must occur on this catalyst, leading in due course to the utilization of previously unexposed catalyst at the pore bottom. With very large particles, when heavily poisoned after a long time, diffusion through this length of poisoned pore may become rate controlling and the activation energy will fall to a low value and the order with respect to hydrocarbon will rise to unity. The pellet sizes used in this work were apparently not great enough to approach this condition. If this situation did arise, it would not affect the poisoning rate since the steam:distillate ratio would be little modified in the absence of reaction by diffusion through an inactive length of pore.

The zone length for the unpoisoned catalyst can be quite long when operating in the regime in which gasification rate is proportional to diameter and the rate of progression of the zone through the bed as poisoning occurs will be that much lower initially than for small particles, since active area not at first used for gasification at the pore bottoms must be used up. Poisoning rates as determined from the progression curves will only be comparable between large particles and small when the amount of bed poisoned is reasonably long compared to the original reaction zone length. As pointed out earlier, this might slightly influence the results obtained in 38 cm beds (Fig. 10 and compare Table 4) but not the results in 84 cm beds (Fig. 11) which showed that catalyst life increased by six times and more in moving from powders to large pellets. As discussed above, operation with large pellets will at most change the average hydrocarbon:steam ratio over the active surface to around 1:3.0 by weight when the inlet ratio is 1:1.66. Figure 10 shows that a change of this order in feed ratio will little more than double the catalyst resistance to poisoning; so it seems that there must be other factors apart from hydrocarbon:steam ratio, which improve the resistance of larger particles.

It can be speculated that the further improvement in resistance arises from the change in the temperature profile observed with large particles, particularly in the endothermic region where the initial temperature fall in the reaction zone seen with powders is virtually absent. The pore diffusion of reactant hydrocarbon and the resultant modification of concentration, which has been discussed represents a drastic oversimplification of a complex reacting system in the pore in which a net pressure change occurs, equilibrium among the gases is approached and gaseous products diffuse outwards as reactants diffuse in. The gases towards the bottom of the pore will approach the composition required by equilibrium at complete hydrocarbon gasification and a temperature profile will no doubt exist down each pore in large particles of a similar shape to that normally seen in a reaction zone in a bed of small particles. These gases will diffuse outwards giving the equivalent of recirculation within the pore. Pore recirculation itself, divorced from its effects on gas temperature, may not have too much influence in suppressing poisoning, but there is no doubt that the gases leaving the pore contain more methane at low conversions and the gases are closer to equilibrium than they would be for the same conversion on small particles (see Table 5). Presumably high methane concentrations at equilibrium at the pore bottom in the absence of residual hydrocarbon do not react quickly enough as they pass out to produce, at the conditions at the pore exit, the hydrogen-rich composition observed on small particles. Probably this is because other higher hydrocarbon molecules occupy most of the active sites preferentially in this region of the pore as they must if the surface reaction is approximately zero order in hydrocarbon. Increased methane means more heat release and as observed the endothermic dip is nearly eliminated compared with small particles. Poisoning will then be less rapid in this region because its rate falls with increasing temperature. No doubt also, those few sites which are occupied by methane poison much more slowly.

There is indirect evidence from pilot plant operation in long 5 cm diameter tubes using 0.32 cm equant pellets (*3*), which throws some light on the question of whether the diffusional barrier is in the micropore or the macropore. Contrary to laboratory experience with 18–30 BSS powders, it was found that the resistance to poisoning of the pelleted catalyst fell somewhat as the total pressure of operation rose from 25 to 69 atm; whereas, resistance rose markedly when the operating pressure was 10 atm. This favors reaction rate control in the micropores with Knudsen diffusion, at least at the lower pressures, for then h is inversely proportional to the root of the hydrocarbon pressure (the overall order is 0.5). As pressure is increased, h falls and hydrocarbon concentrations at the bottom of the pores will rise for a given particle size and structure and the average hydrocarbon:steam ratio over the active surface will increase, leading to more rapid poisoning. Of course the poisoning rate will not continue to increase with pressure, for, beyond a certain point, bulk diffusion will limit the rate in the micropores and h will be independent of the pressure. These conclusions were supported by the observation that the length of the reaction zone as shown by the temperature profile, a very approximate measure of reaction rate, tended to shorten as the pressure was raised, indicating that the overall reaction order was greater than zero for pellets. From the point of view of plant operation these observations show that great care is required in selecting the optimum particle size for long catalyst life in this pressure region, since rises in h caused by pressure can be offset by increases in particle diameter as long as pressures are such that Knudsen diffusion is rate controlling.

The improved resistance of the catalyst to poisoning as a consequence of the diffusional barrier will be lost as the barrier is removed. This phenomenon shows itself in plant operations. For the first few hundred hours on stream, the endothermic dip is largely absent; but, as time progresses, it begins to develop slowly. Continuous slow sintering of unutilized catalyst in product gases causes a progressive though small loss of area, perhaps by coalescence of micropore structure, which will reduce K_gN_0. At the same time the radius of the micropores tends to increase (*4*) as a result of heat treatment. Both these effects reduce h for a given particle diameter. After some thousands of hours, depending on the diameter, the dip becomes very large and thereafter the poisoning of the remainder of the catalyst bed is much more rapid and similar in rate to that observed on powdered catalyst.

CONCLUSIONS

The present results show that the ideal conditions of operation for a low-temperature-supported nickel gasification catalyst represent a compromise. If operating temperature is too low, catalyst poisoning by hydrocarbon molecules will be more rapid, if too high, excessive active surface will be lost through sintering and the possibility will increase of carbon deposition by the Boudouard equilibrium and perhaps also by hydrocarbon pyrolysis. Higher feed steam:hydrocarbon ratios reduce poisoning, but these are only obtained on plant at the expense of thermal efficiency. Low boiling distillates are advantageous but may be more costly. The use of large-sized catalyst particles improves resistance to poisoning without changing overall feed ratio or operating temperature, as a consequence of diffusional limitations on the reaction rate and the associated changes for the better in temperature and steam:hydrocarbon ratio.

ACKNOWLEDGMENT

The authors thank the Gas Council for permission to publish this paper.

REFERENCES

1. COCKERHAM, R. G., PERCIVAL, G., AND YARWOOD, T. A., *Inst. Gas Eng., J.* **5**, 109 (1965).
2. PHILLIPS, T. R., YARWOOD, T. A., MULHALL, J., AND TURNER, G. E., *J. Catal.* **17**, 28 (1970).
3. DAVIES, H. S., unpublished data.
4. WILLIAMS, A., BUTLER, G. A., AND HAMMONDS, J., to be published by *J. Catal.*
5. KERLEY, W., unpublished data.
6. PHILLIPS, T. R., MULHALL, J., AND TURNER, G. E., *J. Catal.* **15**, 233 (1969).
7. WHEELER, A., *Advan. Catal. Relat. Subj.* **3**, 250 (1951).
8. VAN ZOONEN, D., *Proc. Int. Congr. Catal. 3rd, 1964* **2**, 1319 (1965).